Computer Methods and Programs in Biomedicine 216 (2022) 106677

Contents lists available at ScienceDirect

Computer Methods and Programs in Biomedicine

journal homepage: www.elsevier.com/locate/cmpb

Application of photoplethysmography signals for healthcare systems: An in-depth review

Hui Wen Loh[a], Shuting Xu[b,d], Oliver Faust[c], Chui Ping Ooi[a], Prabal Datta Barua[d,e], Subrata Chakraborty[f,g], Ru-San Tan[h,i], Filippo Molinari[j], U Rajendra Acharya[a,e,k,l,m,*]

[a] School of Science and Technology, Singapore University of Social Sciences, Singapore
[b] Cogninet Australia, Sydney, New South Wales 2010, Australia
[c] Department of Engineering and Mathematics, Sheffield Hallam University, Sheffield S1 1WB, United Kingdom
[d] Faculty of Engineering and Information Technology, University of Technology Sydney, Australia
[e] School of Business (Information Systems), Faculty of Business, Education, Law and Arts, University of Southern Queensland, Australia
[f] School of Science and Technology, Faculty of Science, Agriculture, Business and Law, University of New England, Armidale, NSW 2351, Australia
[g] Centre for Advanced Modelling and Geospatial Information Systems (CAMGIS), Faculty of Engineering and Information Technology, University of Technology Sydney, Sydney, NSW 2007, Australia
[h] Department of Cardiology, National Heart Centre Singapore, 169609, Singapore
[i] Duke-NUS Medical School, 169857, Singapore
[j] Department of Electronics and Telecommunications, Politecnico di Torino, Italy
[k] School of Engineering, Ngee Ann Polytechnic, 535 Clementi Road, 599489, Singapore
[l] Department of Bioinformatics and Medical Engineering, Asia University, Taiwan
[m] Research Organization for Advanced Science and Technology (IROAST), Kumamoto University, Kumamoto, Japan

ARTICLE INFO

Article history:
Received 2 December 2021
Revised 30 January 2022
Accepted 30 January 2022

Keywords:
Photoplethysmography (PPG)
Deep learning
Machine learning
PRISMA
Cardiac
Blood pressure
Sleep
Mental health
Diabetes
Computer-aided diagnosis (CAD)

ABSTRACT

Background and objectives: Photoplethysmography (PPG) is a device that measures the amount of light absorbed by the blood vessel, blood, and tissues, which can, in turn, translate into various measurements such as the variation in blood flow volume, heart rate variability, blood pressure, etc. Hence, PPG signals can produce a wide variety of biological information that can be useful for the detection and diagnosis of various health problems. In this review, we are interested in the possible health disorders that can be detected using PPG signals.
Methods: We applied PRISMA guidelines to systematically search various journal databases and identified 43 PPG studies that fit the criteria of this review.
Results: Twenty-five health issues were identified from these studies that were classified into six categories: cardiac, blood pressure, sleep health, mental health, diabetes, and miscellaneous. Various routes were employed in these PPG studies to perform the diagnosis: machine learning, deep learning, and statistical routes. The studies were reviewed and summarized.
Conclusions: We identified limitations such as poor standardization of sampling frequencies and lack of publicly available PPG databases. We urge that future work should consider creating more publicly available databases so that a wide spectrum of health problems can be covered. We also want to promote the use of PPG signals as a potential precision medicine tool in both ambulatory and hospital settings.

1. Introduction

A typical photoplethysmography (PPG) device consists of a light source and a photodetector to perform a non-invasive assessment of the blood volume changes in the microcirculation of an accessible body part, e.g., pulp of the fingertip. The PPG waveform, like electrocardiography (ECG), provides information on the heart rate. The difference between an ECG and PPG waveform is depicted in Fig. 1. The ECG estimates the heart rate based on the electrical signal conduction within the heart during the cardiac cycle. The P wave, QRS complex, and T wave represent depolarization of the atria (atrial systole), depolarization of the ventricles (ventricular systole), and repolarization of the ventricles (ventricular diastole), respectively [1]. In other words, depolarization and repolarization mark the start of contraction and relaxation of the heart muscle, respectively.

* Corresponding author at: School of Engineering, Ngee Ann Polytechnic, 535 Clementi Road, 599489, Singapore.
E-mail address: aru@np.edu.sg (U.R. Acharya).

https://doi.org/10.1016/j.cmpb.2022.106677

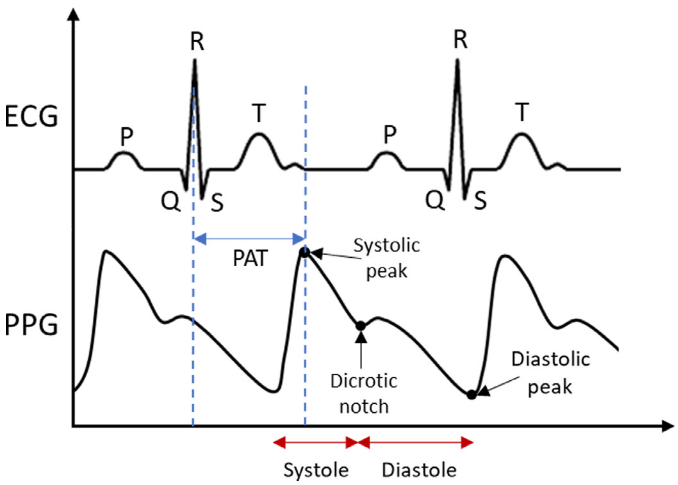

Fig. 1. Schematic drawing of ECG and PPG waveforms.

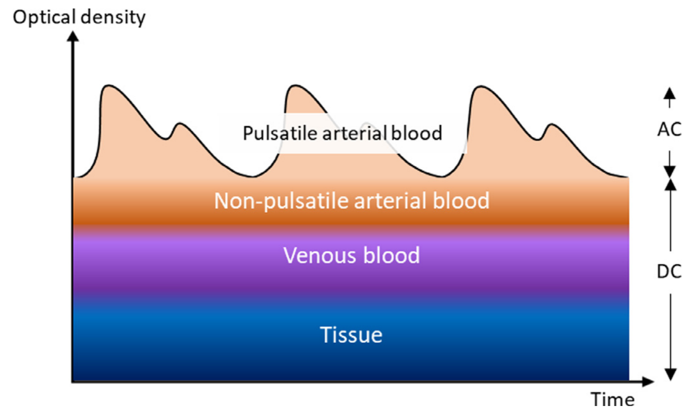

Fig. 3. Schematic drawing of the AC and DC components of PPG signal.

In contrast, the PPG estimates the heart rate by measuring the amount of light absorbed or reflected by the pulsatile blood flow within the vessels [2]. As the heart contracts, the rapid increase of blood flow volume in the arteries, veins, and capillaries attenuates the light source of the PPG measuring device, allowing it to detect the changes in blood flow volume during the cardiac cycle. The PPG waveform consists of three main events: systolic peak, dicrotic notch, and diastolic peak. The systolic and diastolic peaks indicate detection of the transmitted ventricular contraction and relaxation at the measurement site, while the dicrotic notch is caused by the closure of the aortic valve, which indicates the end of the systole phase and beginning of the diastole phase [3] (Fig. 1). The pulse arrival time (PAT) as indicated in Fig. 1, is the time taken for the pulse from the heart to reach the PPG measurement site.

Although ECG is the gold standard for heart rate measurement, PPG offers an expedient alternative that the lay public can use to assess their health status immediately [4,5]. The ECG procedure requires the exact placement of chest electrodes (Fig. 2), which the public is not familiar with [5,6]. As a wearable device, a protruding ECG device under the shirt may be cumbersome and uncomfortable. This limits the uptake of portable ECG devices as wearable consumer health technology. On the other hand, smartphones, and smartwatches nowadays are equipped with PPG measuring devices (Fig. 2). It is no longer necessary for people to purchase standalone oximeters when PPG measurements can be easily obtained using ubiquitous mobile devices.

The PPG signals contain a wide range of physiological information that can play an important role in the detection of abnormal health status in both ambulatory and hospital settings [5,7]. The PPG waveform comprises pulsatile (AC) and non-pulsatile (DC) components [7,8] (Fig. 3). The AC component provides information on volumetric changes in blood vessels, which corresponds to the heart rate (Fig. 1). The DC component measures light absorbed by the tissue, veins, and blood at the measuring site, which informs on the volume capacity in the blood vessels, such as changes in the venous capacity because of respiration [8].

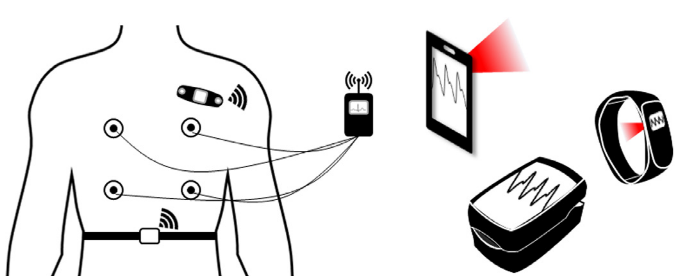

Fig. 2. Examples of wearable ECG devices (left) and PPG devices (right).

The abundance of physiological information offered by PPG signals prompts research into a diversity of health conditions. Notably, researchers have employed artificial intelligence (AI) techniques to learn PPG characteristics for automated detection of disease. In this work, we review studies that used statistical, machine learning, and deep learning approaches to using PPG signals computer-aided diagnosis (Fig. 4). It may be noted that in Fig. 4, PPG signals need to be preprocessed to denoise the signal via motion artifact reduction methods before it can be used. In the first route (statistical), coefficients are computed from extracted PPG features and compared to reference values, and then classified as normal or abnormal signals. In [9] a PPG-derived apnea-hypopnea index above 15 indicated moderate disease severity among 48 subjects with suspected obstructive sleep apnea. In the second route (machine learning), features are extracted from the PPG signal (e.g., PAT, systolic peaks, blood flow volume, etc.) and significant ones selected to be fed to a classifier. Feature selection is a mandatory step in machine learning [10]. Plagued with the curse of dimensionality, machine learning classifiers cannot process high-dimensional data like PPG signals in their raw form [11]. Feature extraction and selection reduce dataset dimensions, thereby preventing overfitting by classifiers [12]. Common machine learning classifiers include support vector machine (SVM) [13], random forest (RF) [14], logistic regression (LR) [15], k-nearest neighbor (KNN) [16], and artificial neural network (ANN) [17]. In deep learning, the PPG signal and/or extracted features are fed to a neural network classifier which mimics the brain's neural connectivity [18] without the need for feature selection [10,12]. A typical deep learning model comprises an input layer, multiple hidden layers, and an output layer. The input layer reads the PPG signal and/or extracted feature, preprocesses it, and forwards the processed information to a series of hidden layers. The hidden layers assess the information collected from the input layer or the layer before it (multiple hidden layers), recalculate the information, and forward it to the output layer where classification is performed. Each layer contains neurons (symbolized by the black dots in Fig. 4) that compute output values from the weights that lie in the connections between the neurons (symbolized by the black lines in Fig. 4) [18]. The model learns the characteristics of the PPG signals by processing labeled training dataset samples repeatedly, which allows the weights of the connections between neurons to update iteratively. Unlike machine learning, deep learning models are capable of learning PPG signals in their raw form as the multiple hidden layers, which earn them the appellation "deep" [10], allow them to learn data of high

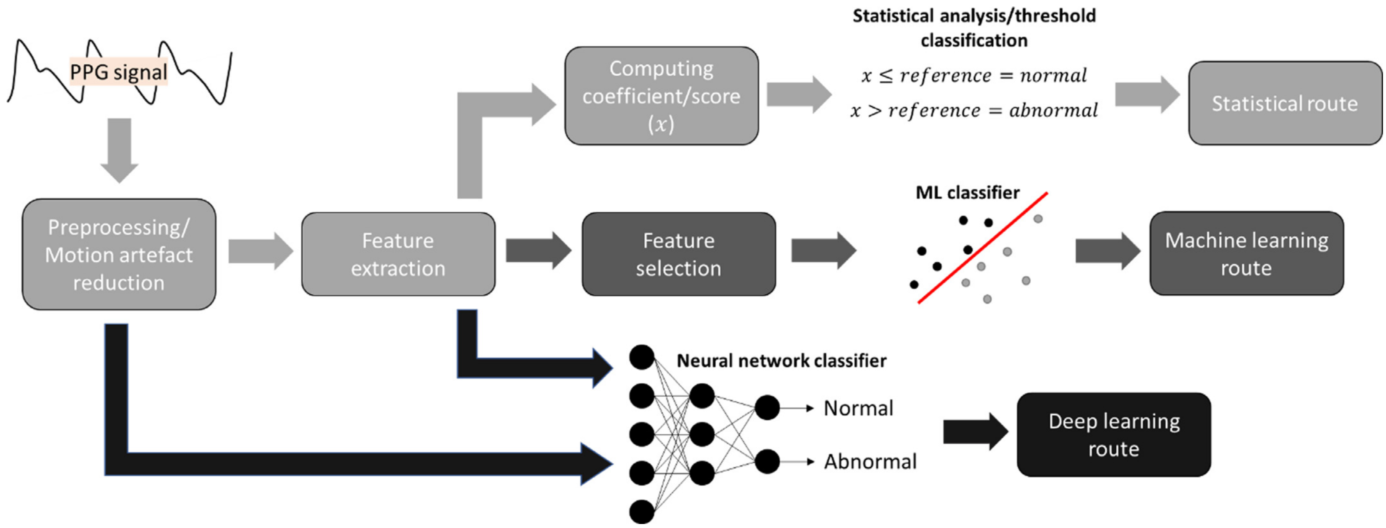

Fig. 4. Three approaches for computer-aided diagnosis using PPG signals.

Table 1
Boolean search string for the respective journal databases.

Database	Boolean search [Title]	Boolean search [Title/Abstract]	No. of results
PubMed	"Photoplethysmography"	"detection" and "deep learning" "detection" and "machine learning" "diagnosis" and "deep learning"	63
IEEE		"diagnosis" and "machine learning" "prediction" and "deep learning" "prediction" and "machine learning"	15
Science direct		"detection" or "deep learning" "detection" or "machine learning" "diagnosis" or "deep learning" "diagnosis" or "machine learning" "prediction" or "deep learning" "prediction" or "machine learning"	115
Google scholar		"detection" or "diagnosis" or "identification" or "prediction" or "deep learning" or "machine learning"	268

complexities. Common deep learning models include deep neural network (DNN) [19], convolutional neural network (CNN) [20], recurrent neural network (RNN) [21], and long short-term memory (LSTM) [22].

2. Methods

We performed a literature search of studies related to AI techniques in PPG that had been published from Jan 2011 to October 2021 on the following databases: Institute of Electrical and Electronics Engineers (IEEE) Xplore Digital Library, PubMed, Science Direct, and GOOGLE Scholar using search terms that are listed in Table 1. 461 articles were retrieved with initial screen, which was reduced to 43 studies after filtering out 121 duplicate papers, 242 non-assessable publications (available only in a non-English language, abstract, or conference formats), and 55 papers that failed relevancy checks. Fig. 5 depicts the PRISMA [23] workflow of the literature search.

3. Results

There was 25 health issues identified from the 43 studies that are eligible for this review, of which 14, 8, 7, 6, 2, and 6 PPG studies related to cardiac, blood pressure, sleep, mental, diabetes, and miscellaneous health issues. Details of all these studies are listed in Table A.1.

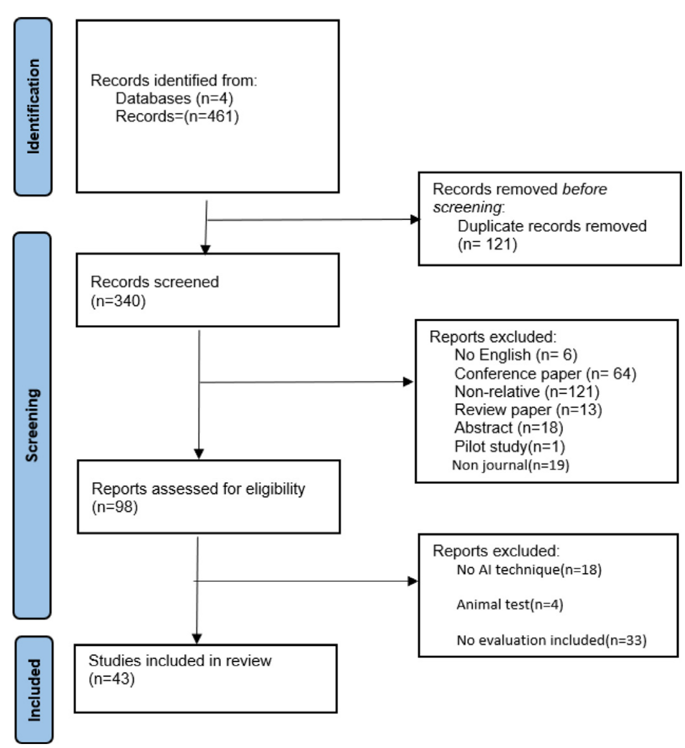

Fig. 5. PRISMA flow chart.

3.1. Cardiac

Half of the cardiac studies were on atrial fibrillation (AF) diagnosis with PPG signals [24–30], and the remainder evenly split among premature ventricular contraction (PVC) [17], peripheral arterial disease (PAD) [31], malignant ventricular arrhythmias (MAS) [14], coronary artery disease (CAD) [32], aortic aneurysm [33], cardiovascular [34] risk and cardiomyopathy [35] detection. Among these, 4, 7, and 3 studies were based on algorithm approach [24,27,29,30], machine learning [14,17,25,32–35], and deep learning [26,28,31], respectively, for disease prediction.

Only 12 studies provided details of one or more performance metrics (accuracy, sensitivity, and specificity) for comparison of model performance (Fig. 6). For AF diagnosis, the algorithm approach yielded the most favorable results, with reported high 97% accuracy [27,29,30], sensitivity 95.4–100% [24,27,29,30] and specificity 96–99.7% [24,27,29,30]. The machine learning studies that reported detailed performance include those that used PPG signals for assessment of PVC (ANN classifier) [17], MAS (RF classifier) [14], aortic aneurysm (KNN classifier) [33], cardiovascular risk level (Gaussian mixture model) [34], and various cardiomyopathies (kernel k-means classifier) [35]. Except for [33], which reported a classification accuracy of 60% for detection of aortic aneurysm, the rest of the machine learning studies attained high performance: 97.9–100% accuracy [17,34,35], 89–100% sensitivity [14,17,25,34,35], and 93.3–100% specificity [14,17,25,34]. Among deep learning studies, two used CNNs, which are preferred models for recognition of high-dimensional raw PPG signal characteristics, to detect AF [26,28]. One study [31] converted PPG signals into spectrograms images that were then input to a hybrid CRNN model (combination of CNN and RNN models), and attained high accuracy 88.9%, sensitivity 86.6%, and specificity 90.2% for detection of PAD.

3.2. Blood pressure

The PPG studies of blood pressure involved detection of hypertension [20,36,37], hypotension [38,39], both hypertension and hypertension [40], as well as specific medical emergencies like pregnancy-associated preeclampsia [15] and heart failure-induced mechanical alternans [41] that are characterized by extreme blood pressure perturbations. Among these, 1, 3, and 4 studies were based on statistical approach [41], machine learning [15,38,40], and deep learning [20,36,37,39], respectively, for disease prediction. The performance metrics are depicted in Fig. 7.

In [36], a deep learning model that used PPG to detect hypertension yielded 90% accuracy. For detecting hypotension, [38] and [39] employed machine learning and deep learning, respectively. The former achieved superior 94.5% accuracy, 91.7% sensitivity, and 95.8% specificity [38] using an AdaBoost classifier. In [40], using PPG signals fed to an SVM classifier to detect both hypertension and hypotension yielded poor classification accuracy of 60%. In [41], an algorithm approach was used to detect mechanical alternans, i.e., alternating weak and strong heartbeats in succession, associated with heart failure, based on 8 heart rate variability (HRV) features extracted from PPG signals. Each HRV feature had its own designated threshold. For instance, pulse width had a threshold range of 22–23%; and pulse interval, 0–3. This proposed algorithm achieved an average accuracy of 98%. In [15], a machine learning-based logistic regression classifier was used to diagnose preeclampsia on PPG signals with promising 87.5% accuracy, 83.3% sensitivity, and 91.0% specificity. Preeclampsia is a rare but serious pregnancy complication in which the mother develops severe hypertension and organ failure. Failure to detect and intervene may result in maternal and fetal death [42], which underscores the use case for the PPG monitoring in high-risk pregnancies.

3.3. Sleep health

In this review, five PPG studies involved the detection of obstructive sleep apnea (OSA) [9,16,21,43,44]; and two, sleep stages classification [19,22]. Among these, 1, 3, and 3 studies were based on statistical approach [9], machine learning [16,43,44], and deep learning [19,21,22], respectively, for disease prediction. The performance metrics are depicted in Fig. 8.

OSA occurs when the throat muscle relaxes during sleep and narrows the airway, thereby blocking normal airflow and causing the individual to suffer interrupted breathing during sleep. In [44], a machine learning-based ensemble classifier attained 95% accuracy, 93% sensitivity, and 96% specificity for OSA diagnosis. For sleep stage classification, Radha et al. [22] used a deep LSTM model to classify sleep stages into sleep and wake stages with 76.4% accuracy, while Walch et al. [19] used a DNN model to perform more granular 4-class classification into the wake, rapid-eye-movement, light, and deep sleep stages with 77.4% accuracy

3.4. Mental health

PPG signals can also be used to assess the mental welfare of an individual. The PPG studies of mental health involved detection of mental stress [45–48], panic disorder [49], and emotional eating [50]. Among these, 4 and 2 studies were based on machine learning [45,47,49,50], and deep learning [46,48], respectively. The performance metrics are depicted in Fig. 9.

Mental stress is a psychological response to stressors such as fear, pain, or change in the environment. Long-term stress can induce depression and anxiety [46], as well as sleep problems and cardiac disease [51]. Among PPG studies on mental stress detection, Elzeiny and Qaraqe [46] achieved the highest classification accuracy of 98.5% with a deep learning model. Panic disorder is characterized by episodes of panic attacks such as dizziness, shortness of breath, and trembling. In [49], the authors input PPG-derived HRV to a machine learning route LR classifier and attained fair 78.4% accuracy, 83.3% sensitivity, and 73.3% specificity for detection of panic disorder. In emotional eating, the patient eats to fill an emotional void and generate a false sense of "fullness" [50], which can lead to unhealthy binge eating and bulimia [52]. In [50], PPG-derived HRV was input to a machine learning SVM classifier to detect emotional eating with 78% accuracy, 78.8% sensitivity, and 75% specificity.

3.5. Diabetes

In the review, there are only two studies that used PPG to detect diabetic peripheral neuropathy [53,54], a complication of chronic diabetes mellitus. In diabetes, there are abnormally high blood glucose levels [55] that over time damage microcirculatory blood vessels, inhibit transport of nutrients to the nerves, and result in nerve damage, which manifests as loss of sensation in the limbs, especially the feet [56]. Both studies used machine learning (Table 2). The better performance (outstanding 99.9% accuracy, sensitivity, and specificity) was seen with [53], in which Mel frequency cepstral coefficients (compact representations of the PPG signal in the amplitude domain) were extracted from PPG signals and input to hybrid feature selection-based XGBoost system.

3.6. Miscellaneous

In the review, six PPG studies involved miscellaneous conditions (Table 3). Cerebral artery stenosis is usually diagnosed on imaging, e.g., magnetic resonance or computer tomographic angiography. In [57], PPG signals from treatment and control groups were input to a machine learning linear discriminant analysis (LDA)

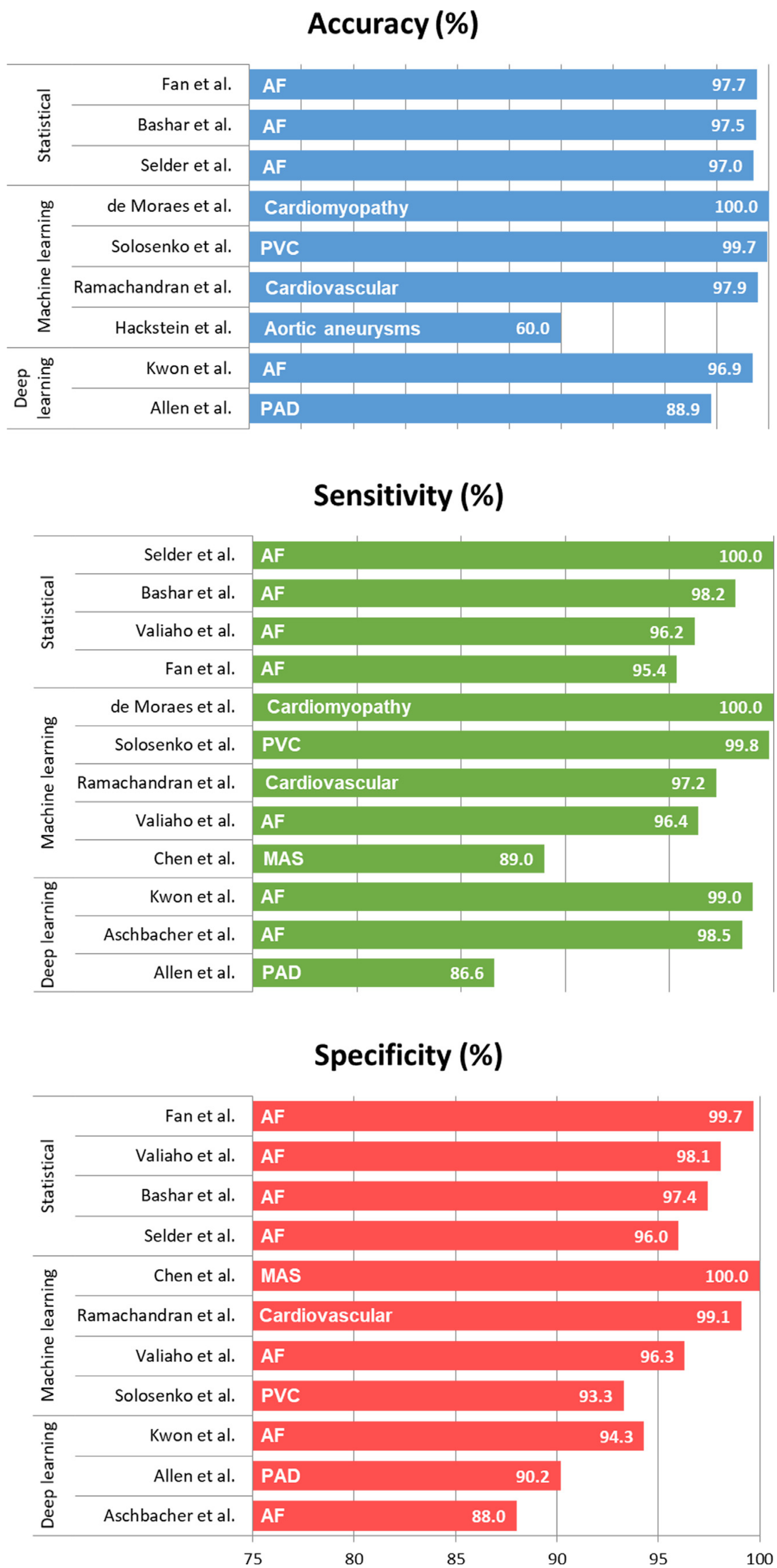

Fig. 6. Bar chart representation of the performance metrics provided by PPG studies in the cardiac category. AF – atrial fibrillation, PVC - premature ventricular contraction, MAS - malignant ventricular arrhythmias, and PAD - peripheral arterial disease.

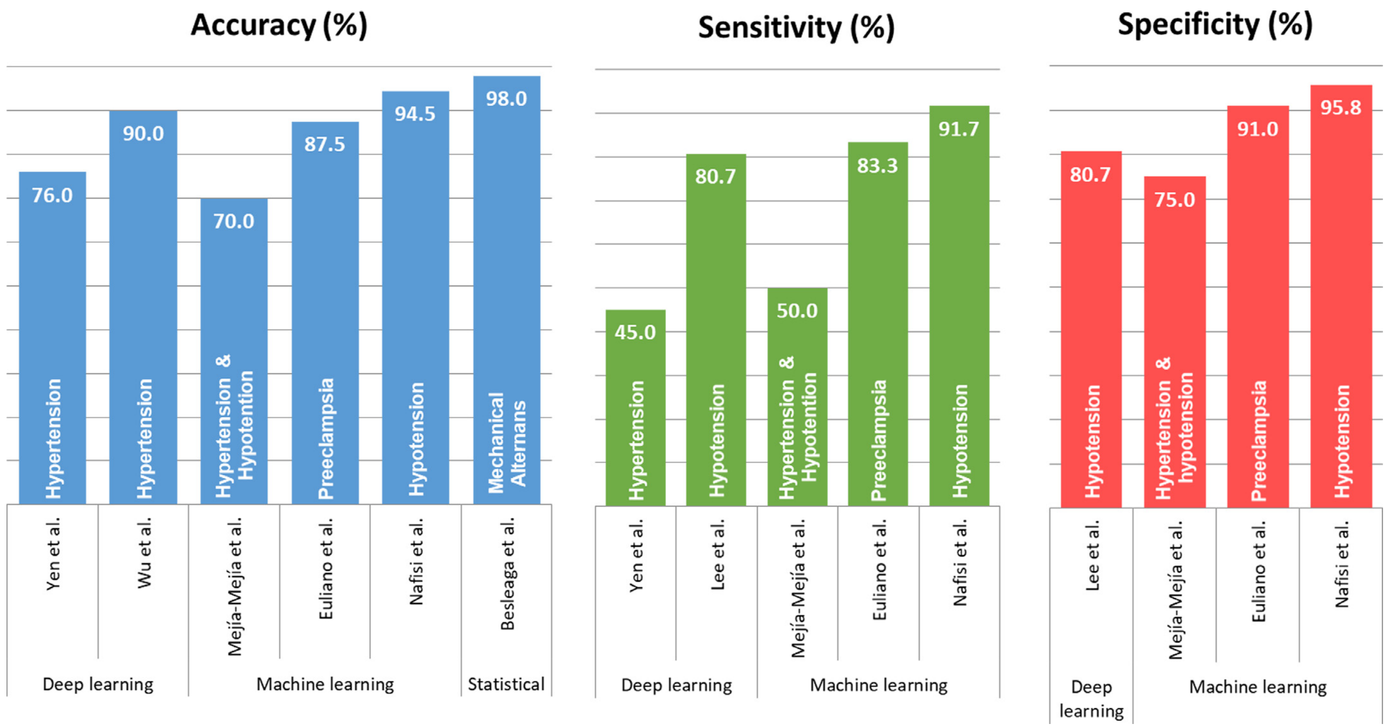

Fig. 7. Bar chart representation of the performance metrics provided by PPG studies in the blood pressure category.

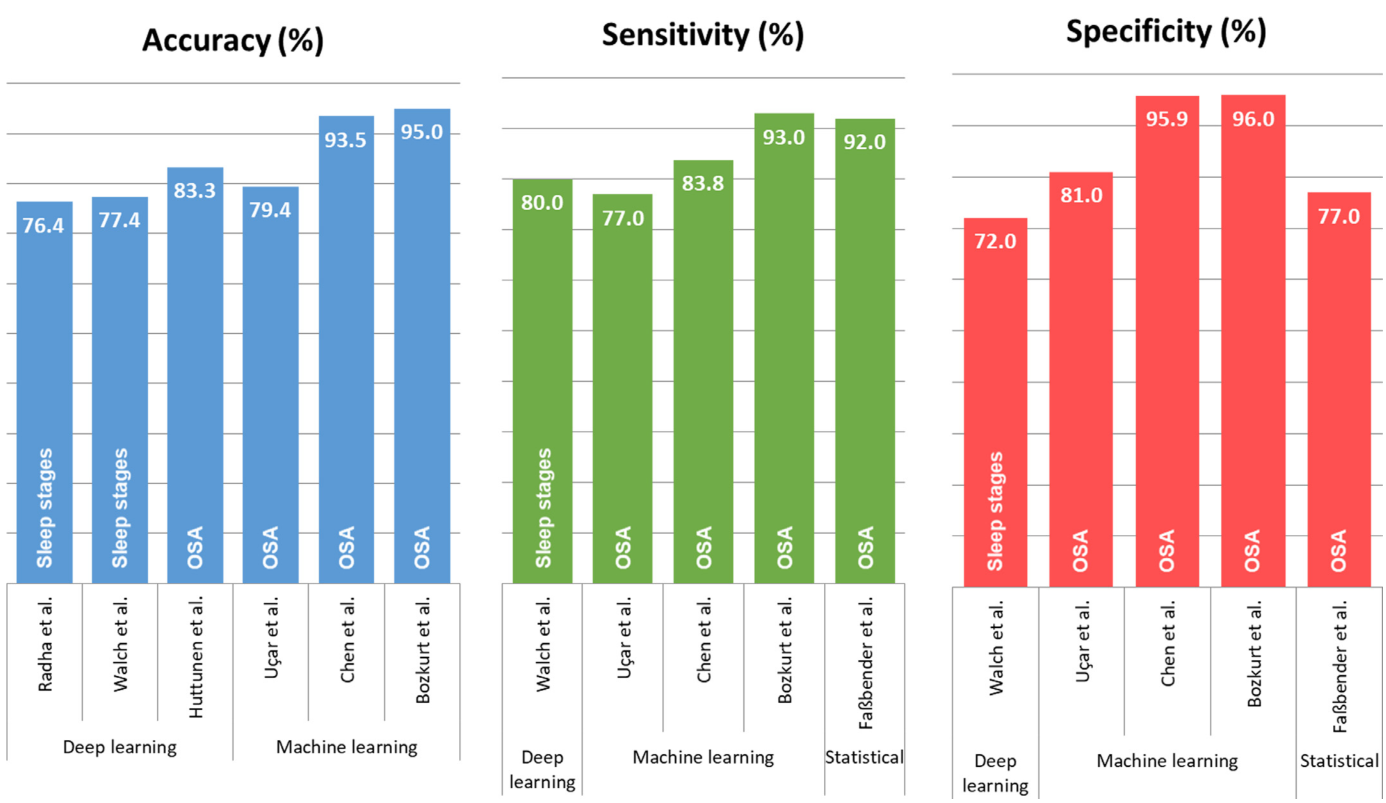

Fig. 8. Bar chart representation of the performance metrics provided by PPG studies in the sleep health category. OSA – obstructive sleep apnea.

Table 2
Details of PPG studies in the diabetes category.

Refs.	Subcategory	Feature extracted	Route (classifier)	Accuracy	Sensitivity	Specificity
Prabha et al. [53]	Diabetes mellitus	PPG waveform	ML (Hybrid FS-based XGBoost system)	99.9%	99.9%	99.9%
Xiao et al. [54]	diabetic peripheral neuropathy	HRV	ML (Logistic regression)	78.2%	–	–

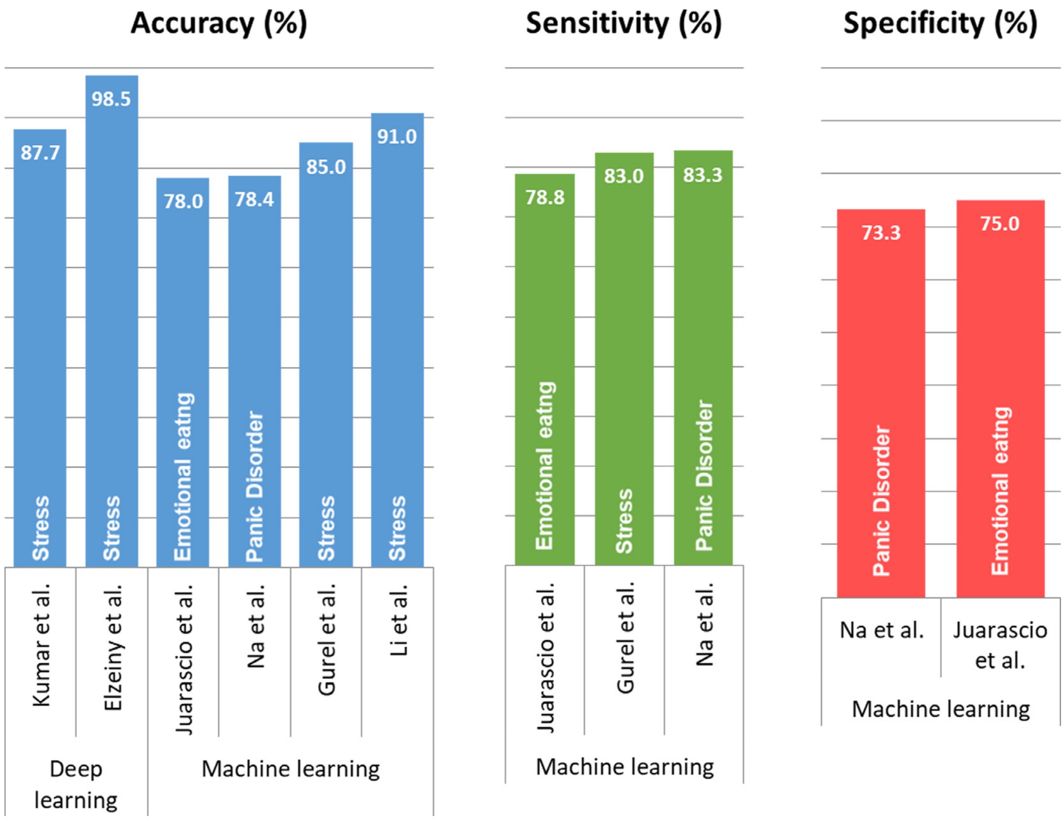

Fig. 9. Bar chart representation of the performance metrics provided by PPG studies in the mental health category.

Table 3
Details of PPG studies in the miscellaneous category.

Refs.	Subcategory	Feature extracted	Route (classifier)	Accuracy	Sensitivity	Specificity
Kang et al. [57]	Cerebral artery stenosis	PPG components	ML (LDA)	92.2%	90.6%	93.8%
Chiang et al. [13]	Arteriovenous fistulas	PPG components	ML (SVM)	88.6%	–	–
Roy Chowdhury et al. [58]	Anesthesia	PPG waveform	DL (CNN)	86.0%	–	–
Lim et al. [59]	Pain	HRV	DL (DBN)	65.6%	–	–
Bourdillon et al. [60]	Sports: overreaching	PPG waveform	Statistical (statistical analysis)	–	–	–
Ouyang et al. [61]	Comorbid: CAD & atherosclerosis	HRV	ML	–	–	–

classifier and yielded high classification accuracy, sensitivity, and specificity of 92.2%, 90.6%, and 93.8%, respectively [57]. In chronic kidney disease patients, arteriovenous fistulae are surgically created between veins and arteries for access during hemodialysis treatment. Many complications can occur at the site of arteriovenous fistulae like thrombosis, calcification, and inflammation, which interfere with the hemodialysis treatment [13]. In [13], the authors assessed the quality of arteriovenous fistulae by inputting PPG-derived blood flow volumes (BFV) from study participants into a machine learning SVM classifier, which classified the signals into negative (BFV $<$ 600 mL/min) and positive classes (BFV $>$ 600 mL/min), and obtained 88.6% accuracy.

There is no standard measurement for anesthesiologists to assess the anesthetic state in an anesthetized patient during surgery. In [58] the authors used a deep learning CNN model to perform a 3-class classification of the anesthetic state (deep, okay, and light). They produced heatmaps from PPG and ECG signals to train their proposed CNN model and achieved an accuracy of 86%. In another study, [59], the authors used deep learning (deep belief network) to assess the level of pain during anesthesia but attained only modest 65.6% accuracy.

Bourdillon et al. [60] used PPG signals to detect overreaching in athletes. This is caused by the imbalance between physical training and recovery and can result in declining athletic performance despite continual training. In their study, they adopted the statistical route to uncover patterns in the variance of the systolic, diastolic, and dicrotic amplitudes in the PPF signal. They reported that variance was larger in overreached athletes compared with non-overreached but acutely fatigued athletes (no standard performance metric was reported). Lastly, Ouyang et al. [61] employed PPG signals for the detection of comorbidities, namely CAD and atherosclerosis. In their study, they noticed that PPG-derived pulse wave velocities were consistently higher for older subjects than younger subjects in the CAD, hypertensive, and healthy groups. Likewise, no standard performance metric was reported in their study.

4. Discussion

We have surveyed six main categories of conditions in which PPG signals can be applied to detect various health problems. Among these, AF (cardiac), hypertension (blood pressure), OSA (sleep health), and stress (mental health) were the most studied health problems in the respective categories. The rest of the health problems each had less than two PPG studies. One noteworthy PPG AF detection study is that by Bashar et al. [29], which recruited 10 AF subjects and 9 healthy controls. The authors adopted the statistical route and proposed a premature atrial contraction

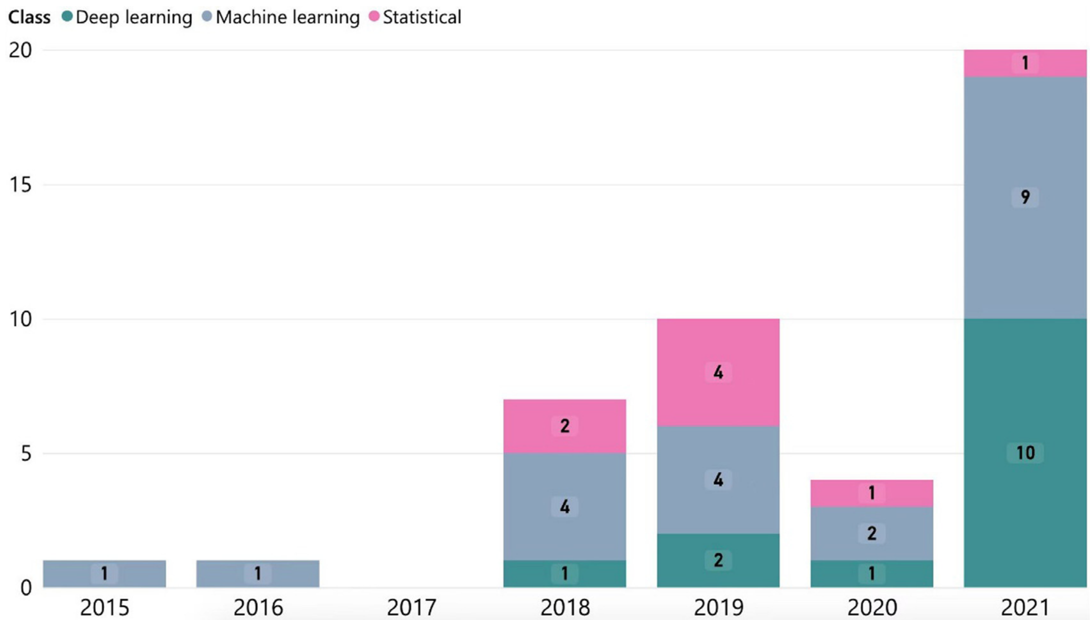

Fig. 10. The number of PPG studies across the years from 2015 to 2021 for the deep learning, machine learning, and statistical route.

detection algorithm, whereby a combined coefficient was computed from two PPG-derived HRV features, sample entropy and root mean square of successive differences. A combined coefficient exceeding a threshold value of 0.94 denoted AF. Among hypertension studies, Wu et al. [36] obtained the highest accuracy using scalograms images of PPG signals to train their deep learning CNN model. Notably, they studied the public database MIMIC-III, which contains 67,830 records from 30,000 intensive care unit patients. Among the PPG studies for OSA diagnosis, Bozkurt et al. [44] obtained the best performance with machine learning ensemble classifier, which gathered the majority voting from various classifiers like KNN, ANN, SVM, and probabilistic neural network that had all been trained on 16 significant features selected from 46 frequency- and time-domain PPG features using F-score algorithm. However, the study had a small sample size of 10 subjects. In the study by Elzeiny and Qaraqe on stress detection [46], healthy participants wore wristband PPG devices while being subjected to stressful tasks, e.g., solving arithmetic problems within 10 min, preparing for a presentation in 5 min. The PPG signals were converted into 2D spatial images and input to a deep learning CNN model for classification.

The increasing secular trend of the use of PPG for the detection of various health problems, especially with machine learning and deep learning, is demonstrated in Fig. 10. Among the different approaches, the statistical route, which is getting less popular, is closer to evidence-based diagnosis and has high levels of explainability, which is not found in many deep learning models due to their black-box nature [10]. Likewise, machine learnings techniques are often coupled with complicated feature engineering and selection processes. The reason why certain features are significant is not apparent, and their clinical relevance may therefore be in doubt [10]. Hence, we caution researchers who are invested in improving the interpretability of machine learning and deep learning not to ignore the statistical approach entirely as it has the potential to decrease the uncertainty in these artificial intelligence models.

Notwithstanding the limited explainability associated with the machine and deep learning, the studies that adopted these routes yielded good performance for the detection of various health problems, with average accuracy, sensitivity, and specificity of 100%, 99.99%, and 87.30%, respectively (Fig. 11).

Table 4
Details on the range of sampling frequency for each PPG feature.

Features extracted	Sampling frequency range (Hz)
HRV	64–500
PPG waveform	20–8000
PPG components	128–2048

Indeed, the majority of the PPG studies in this review had used machine learning classifiers (21 vs. 14 deep learning vs. 8 statistical routes). Fig. 12 summarizes the classifiers employed in the machine learning and deep learning models reviewed. Among machine learning models, SVM (4 studies) was the most popular classifier, followed by LR (3 studies). For deep learning models, CNN was the most popular (6 studies), followed by the hybrid model CRNN (2 studies).

Regarding the type of features PPG studies used to develop the models, 15 studies employed the raw PPG waveform, while 21 used the PPG-derived HRV and 7 used other extracted PPG components. In the former, PPG waveform refers to studies that had employed the whole end-to-end PPG signals to train the model without feature extraction procedure; this is usually adopted by deep learning models. Next, PPG components refer to various features extracted in the DC components of PPG (Fig. 3), such as blood flow volume, PPG amplitude, respiration, etc. Lastly, HRV is the variation between peak-to-peak intervals of the PPG signal and is derived from the AC component of the PPG signals. Typical sampling frequencies used for the collection of PPG signals for each type of PPG feature in the corresponding studies are listed in Table 4. In this review, only two studies used PPG signals that had been sampled over 2000 Hz. PPG signals with a sampling frequency of 8000 Hz were employed by Fathieh et al. [32], while Hackstein et al. [33] used PPG signals sampled at 2048 Hz. Hackstein et al. [33] detected aortic aneurysms using kNN classifier, and attained a classification accuracy of 60%. Fathieh et al. [32], on the other hand, did not report model accuracy result in their study on detection of CAD with Elastic Net. Hence, it is likely that PPG signals with sampling frequency exceeding 2000 Hz are oversampled and unlikely to provide incremental benefit for disease detection.

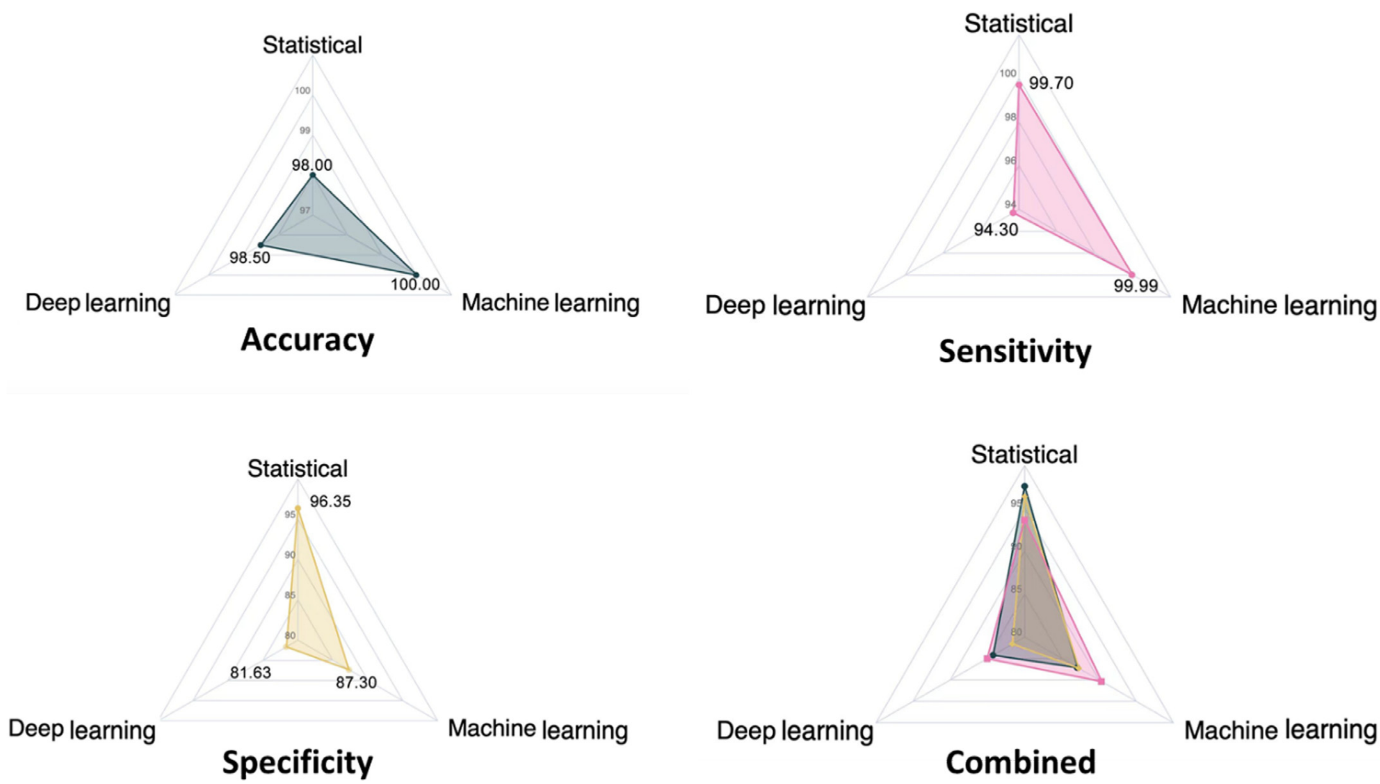

Fig. 11. Radar plot of the average accuracy, sensitivity, specificity, and combined performance metrics gathered from PPG studies in each respective route.

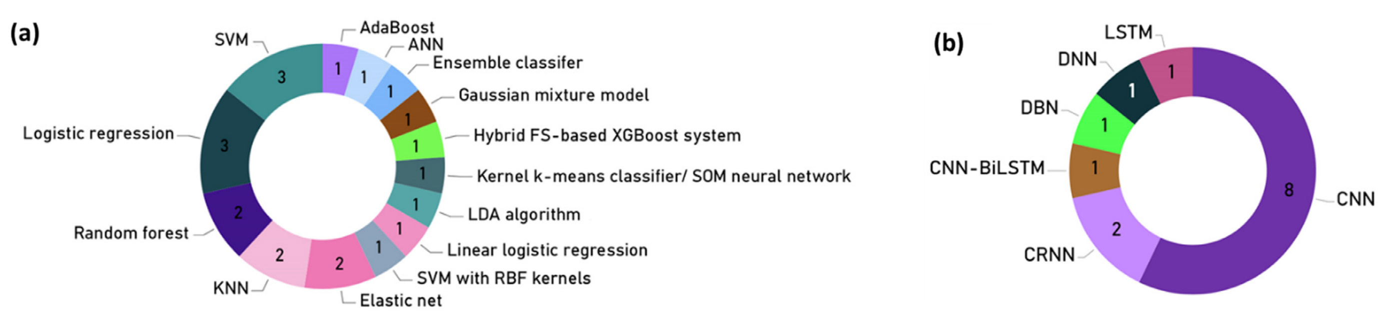

Fig. 12. Pie chart representation of (a) all the machine learning classifiers and (b) deep learning models proposed by PPG studies.

5. Significance aspects and limitations

The following are the most important aspects of our review:

1 We identified 43 eligible PPG studies in this review, which concern 25 health issues that can be classified into six disease categories: cardiac, blood pressure, sleep health, mental health, diabetes, and miscellaneous.
2 We also identified three main strategies (statistical, machine learning, and deep learning) that PPG studies adopted for automated detection of these health issues.
3 Under the cardiac category, eight cardiac diseases were studied: AF, PVC, PAD, MAS, aortic aneurysm, cardiovascular risk, and cardiomyopathy. The most studied cardiac disease was AF.
4 There were four health issues in the blood pressure category: hypertension, hypotension, preeclampsia, and mechanical alternans. The most studied health issue in this category was hypertension.
5 There were only two issues studied in the sleep health category: sleep stages and OSA, and the latter was the most studied health condition.
6 Three mental disorders were studied in the mental health category: mental stress, panic disorder, and emotional eating. The most studied disorder was mental stress.
7 Only two disorders were studied in the diabetes category: diabetes mellitus and diabetic peripheral neuropathy.
8 Lastly, there were 6 health issues studied in the miscellaneous category: cerebral artery stenosis, arteriovenous fistulas, anesthesia, pain, overreaching, and comorbid conditions (CAD + atherosclerosis).
9 These studies demonstrate the versatility of PPG signals for the detection of a variety of diseases with high model performance.

Our review also has the limitations:

1 It is challenging to compare performances between various PPG studies as different datasets had been used. The number of subjects and data collection methods varied widely.
2 There was lack of standardization in the collection of PPG signals between studies; large variation is sampling frequency employed during data collection of PPG signals (Table 4). As such, the optimal sampling frequency for data acquisition is not clear.

Table A.1
List of the 43 studies included in this review after systematic filtering following the PRISMA guidelines.

Refs.	Disorder	dataset	Subjects	Feature	Class	Classifier	Acc	Sen	Spe
Cardiac									
Valiaho et al. [24]	AF	Private dataset (Clinical trial)	106 AF 107 Sinus rhythm	HRV	Statistical	AFEvidence		96.2	98.1
Valiaho et al. [25]	AF	Private dataset (Clinical trial)	169 AF 190 Sinus rhythm	HRV	machine learning	Linear logistic regression		96.4	96.3
Chen et al. [14]	Malignant ventricular arrhythmias (Mas)	Public dataset (SVTDB, VFDB, MITDB)	3279 AF 4030 V 3800 MAs	HRV	Machine learning	random forest		88.98	99.99
de Moraes et al. [35]	Cardiomyopathy	Private dataset	32 cardiopathies 10 healthy	HRV	Machine learning	Kernel k-means classifier/SOM neural network	100	100	
Fathieh et al. [32]	CAD	Private dataset	408 CAD positive with stenosis 186 with LVEDP 676 healthy	PPG waveform	Machine Learning	Elastic net			
Solosenko et al. [17]	premature ventricular contraction (PVC)	Public dataset (MIMIC, MIMIC II)	121 ICU records (MIMIC) 32,536 subjects (MIMIC II)	HRV	Machine learning	ANN	99.7	99.8	93.3
Ramachandran et al. [34]	cardiovascular risk level	Public dataset (capnobase)	28 risk of CVD 14 controls	PPG waveform	Machine learning	Gaussian mixture model	97.88	97.24	99.09
Aschbacher et al. [26]	AF	Private dataset	51 AF patients	PPG waveform	Deep learning	CRNN		98.5	88
Allen et al. [31]	peripheral arterial disease (PAD)	Private dataset	80 Vascular disease 134 healthy	PPG waveform	Deep learning	CNN	88.9	86.6	90.2
Hackstein et al. [33]	aortic aneurysms	Private dataset	28 Aneurysm 27 control	PPG components	machine learning	kNN	60		
Fan et al. [27]	AF	Private dataset (clinical trial)	108 consecutive inpatients	HRV	Statistical	statistical analysis	97.72	95.36	99.7
Kwon et al. [28]	AF	Private dataset (clinical trial)	81 persistent AF 19 long standing persistent AF	PPG waveform	Deep learning	CNN	96.9	99	94.3
Bashar et al. [29]	AF	Private datasets (Umass + Chon-lab)	10 AF (Umass) 9 NSR (Chonlab)	HRV	Statistical	premature atrial contraction detection algorithm	97.54	98.18	97.43
Selder et al. [30]	AF	Private datasets	60 patients including 6 AF	HRV	Statistical	Extra tree classifier	97	100	96
Blood pressure									
Euliano et al. [15]	preeclampsia (PE)	Private dataset	37 PE 43 controls	HRV	Machine learning	Logistic regression	87.5	83.3	91
Liang et al. [20]	hypertension	Public dataset (MIMIC)	121 ICU records (MIMIC)	PPG waveform	Deep learning	CNN			
Besleaga et al. [41]	Mechanical alternans	Private dataset	35 patients	HRV	Statistical	Threshold	98		
Nafisi et al. [38]	hypotension	Private dataset	10 patients	PPG components	Machine learning	AdaBoost	94.5	91.7	95.8
Wu et al. [36]	Hypertension	Public dataset (MIMIC)	121 ICU records (MIMIC-III)	PPG waveform	Deep learning	CNN	90		
Lee et al. [39]	hypotension	Public dataset (VitalDB)	3301 surgical patients	PPG waveform	Deep learning	CNN		80.7	80.7

(continued on next page)

Table A.1 (*continued*)

Refs.	Disorder	dataset	Subjects	Feature	Class	Classifier	Acc	Sen	Spe
Yen et al. [37]	Hypertension	Private dataset	253 prehypertension 120 stage 1 hypertension 61 stage 2 hypertension 240 controls	PPG waveform	Deep learning	CNN-BiLSTM	76	45	
Mejía-Mejía et al. [40]	Hypertension & hypotension	Public dataset (MIMIC II)	32,536 subjects (MIMIC II)	HRV	Machine learning	SVM with RBF kernels	70	50	75
Sleep									
Faßbender et al. [9]	OSA	Private dataset	48 surgical patients with established or suspected OSA and scheduled for elective surgery	PPG waveform	Statistical	Threshold AHI >= 15		92	77
Walch et al. [19]	sleep stages	Private training set Public testing set (MESA)	39 subjects (private)	HRV	Deep learning	DNN	77.4	80	72
Chen et al. [43]	OSA	Private dataset	30 OSA	HRV	machine learning	SVM	93.47	83.79	95.91
Radha et al. [22]	sleep stages	Public dataset	292 participants (Siesta) 60 participants (Eindhoven)	HRV	Deep learning	LSTM	76.36		
Huttunen et al. [21]	OSA	Private dataset	3082 suspected OSA	PPG waveform	Deep learning	CRNN	83.3		
Uçar et al. [16]	OSA	Private dataset	10 OSA	HRV	Machine learning	KNN	79.36	77	81
Bozkurt et al. [44]	OSA	Private dataset	10 participants	PPG components	Machine learning	Ensemble classifier	95	93	96
Mental health									
Li et al. [45]	stress	Private dataset	178 participants	HRV	Machine Learning	Elastic net	91		
Juarascio et al. [50]	emotional eating	Private dataset	21 adults with clinically significant emotional eating behaviors	HRV	machine learning	SVM	77.99	78.75	75
Na et al. [49]	panic disorder	Private dataset	60 Panic disorder 61 anxiety	HRV	Machine learning	Logistic regression	78.4	83.3	73.3
Elzeiny et al. [46]	Stress	Private and public dataset	6 private 15 (WESAD)	HRV	Deep learning	CNN	98.5		
Gurel et al. [47]	stress	Private dataset	16 healthy subjects	PPG components	Machine learning	random forest	85	83	
Kumar et al. [48]	stress	Public dataset (WESAD)	15 participants	PPG components	Deep learning	CNN	87.7		
Diabetes									
Xiao et al. [54]	future peripheral neuropathy	Private dataset	63 non-PN 27 PN	HRV	Machine learning	Logistic regression	78.2		
Prabha et al. [53]	diabetes mellitus (DM)	Private dataset	217 Diabetes VS prediabetes VS healthy	PPG waveform	Machine learning	Hybrid FS-based XGBoost system	99.93	99.93	99.94
Miscellaneous									
Chiang et al. [13]	arteriovenous fistulas	Private dataset	Hemodialysis Patients 74 DOS assessment 79 BFV assessment	PPG components	machine learning	SVM	88.61		

(*continued on next page*)

Table A.1 (*continued*)

Refs.	Disorder	dataset	Subjects	Feature	Class	Classifier	Acc	Sen	Spe
Ouyang et al. [61]	coronary arterial disease & atherosclerosis	Private dataset	100 subjects	HRV	Statistical	Machine learning classifier			
			CAD VS Hypertensive VS healthy						
Bourdillon et al. [60]	Sports: overreaching	Private dataset	15 athletes	PPG waveform	Statistical	Statistical analysis			
Lim et al. [59]	Pain	Private dataset	100 patients scheduled for surgery	HRV	Deep learning	DBN	65.57		
Roy Chowdhury et al. [58]	Anesthesia	Private dataset	50 patients during surgical operation	PPG waveform	Deep learning	CNN	86		
Kang et al. [57]	Cerebral artery stenosis	Private dataset	32 treatment	PPG components	Machine learning	linear discriminant analysis (LDA) algorithm	92.2	90.6	93.8
			32 control						

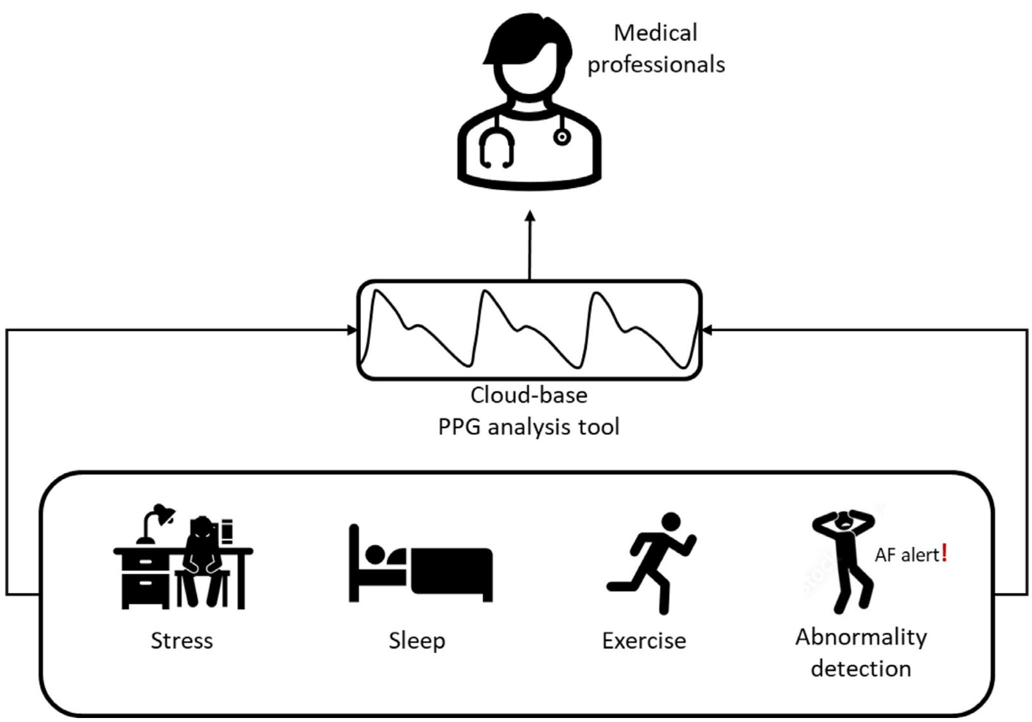

Fig. 13. Block diagram of a cloud-based system for application of PPG signal as precision medicine.

3 The majority of the studies in this review used private datasets (34 studies out of 43 studies, see Table A.1) due to the dearth of large publicly available PPG databases.
4 It is challenging to determine which are the significant PPG features or best performing model for diagnosis as there was a diversity of health issues covered in this review and some of the studies did not report the model performance metrics (i.e., accuracy, sensitivity, and specificity).
5 For instance, in the blood pressure category, the three studies that had investigated hypertension are [20,36,37]. Only [20] and [36] used public database (MIMIC) and [37] had reported model accuracy results [37]. which used private dataset reported model accuracy and sensitivity but have performed multiclass classification instead of binary classification like [36].

6. Future direction

This review surveys the use of artificial intelligence for the analysis of PPG signals for diagnosis in a broad range of health disorders. Some issues need to be addressed to promote future work in this field. Of note, more PPG datasets should be made publicly available. In truth, the process of collecting PPG datasets is a low-cost, convenient, and non-invasive procedure, especially via smartphones and smartwatches. Further, PPG signals demand lower bandwidth, do not consume the battery life excessively [62], and can thus be acquired continuously, which enhances its applicability and optionality in the diagnosis and monitoring of various health states [4].

We aim in our review to promote PPG signals as a potential precision medicine tool of the future. Precision medicine is a tailormade approach whereby medical treatments and interventions are specifically designed to suit an individual's lifestyle, genetic make-up, and environmental variation [63]. The PPG signals can play a part in monitoring lifestyle factors and environmental influences that can affect an individual's health [64]. For instance, a wearable device like smartwatches or a PPG wristband can easily track and record the PPG signal of an individual while he or she is under mental stress, sleeping, and exercising (Fig. 13). These wearable devices would also have access to the cloud where machine learning, deep learning [65–67] or statistical algorithms are stored, and analysis can be performed expeditiously. Individuals would receive alerts when an abnormality is detected, thereby urging him or her to go for medical checkup to confirm if a health abnormality is present. After this, medical professionals can access the patient's data to confirm the diagnosis and prescribe treatment regime that best suit the patient.

7. Conclusion

In this review, we have surveyed health disorders that PPG signals can be used to detect. The different analytical routes used in various PPG studies, namely statistical, machine learning, and deep learning routes, are discussed. We want to highlight the major shortcoming of the PPG studies, which is the lack of accessible public PPG databases despite its low cost and ease of acquisition. In addition, we have also highlighted that PPG signals can be a potential precision medicine tool due to its low bandwidth requirement and measurement complexity, which favor its applicability for remote continuous monitoring and diagnosis. In the future, PPG signals could be an indispensable tool in clinical decision support and lifestyle monitoring in both ambulatory and hospital settings.

Declaration of Competing Interest

The authors declare that they have no conflicts of interest.

U Rajendra Acharya, MTech, Ph.D., DEng, DSc
Ngee Ann Polytechnic, Singapore
Adjunct Professor, University of Malaya, Malaysia
Adjunct Professor, University of Southern Queensland, Australia
Adjunct Professor, Asia University, Taiwan
Associate faculty in SUSS, Singapore
Email: aru@np.edu.sg
Home: https://scholar.google.com.sg/citations?user=8FjY99sAAAAJamp;hl=en
ResearchGate: https://www.researchgate.net/profile/U_Rajendra_Acharya
Publons: https://publons.com/researcher/2836800/rajendra-u-acharya/
Scopus: Author ID: 7,004,510,847
Highly Cited Researcher for *six* consecutive years (2016 to 2021) in Computer Science http://highlycited.com/

Prof. (Dr) Filippo Molinari

Editor in Chief, Computer Methods and Programs in Biomedicine

Sub: Submission of new manuscript to Computer Methods and Programs in Biomedicine

Dear Filippo,

We are submitting the revised manuscript entitled "Application of Photoplethysmography signals for Healthcare systems: An in-depth review" to Computer Methods and Programs in Biomedicine for possible publication. There is no conflict of interest in this work.

Best Regards

U Rajendra Acharya, *M Tech, PhD, DEng,DSc*

Date: 03–12–2021

Declaration of Competing Interest

The authors declare that they have no known competing financial interests or personal relationships that could have appeared to influence the work reported in this paper.

Acknowledgment

NA.

Funding: No funding was received for this study.

Appendix

References

[1] R.G. Carroll, The heart, in: Elsevier's Integrated Physiology, Elsevier, 2007, pp. 65–75.
[2] M. Elgendi, et al., The use of photoplethysmography for assessing hypertension, NPJ Digit. Med. 2 (1) (2019) 60 Dec., doi:10.1038/s41746-019-0136-7.
[3] David Chambers, Christopher Huang, Gareth Matthews, Arterial pressure waveforms, in: Basic Physiology for Anaesthetists, Cambridge University Press, 2019, pp. 155–157.
[4] M. Ghamari, A review on wearable photoplethysmography sensors and their potential future applications in health care, Int. J. Biosens. Bioelectron. 4 (4) (2018), doi:10.15406/ijbsbe.2018.04.00125.
[5] S. Kuntamalla, R.G.R. Lekkala, Quantification of error between the heartbeat intervals measured form photoplethysmogram and electrocardiogram by synchronisation, J. Med. Eng. Technol. 42 (5) (2018) 389–396 Jul., doi:10.1080/03091902.2018.1513578.
[6] J. Li, Q. Ma, A.H. Chan, S.S. Man, Health monitoring through wearable technologies for older adults: smart wearables acceptance model, Appl. Ergon. 75 (2019) 162–169 Feb., doi:10.1016/j.apergo.2018.10.006.
[7] J. Allen, Photoplethysmography and its application in clinical physiological measurement, Physiol. Meas. 28 (3) (2007) R1–R39 Mar., doi:10.1088/0967-3334/28/3/R01.
[8] C. Lee, H.S. Shin, M. Lee, Relations between ac-dc components and optical path length in photoplethysmography, J. Biomed. Opt. 16 (7) (2011) 077012, doi:10.1117/1.3600769.
[9] P. Faßbender, A. Haddad, S. Bürgener, J. Peters, Validation of a photoplethysmography device for detection of obstructive sleep apnea in the perioperative setting, J. Clin. Monit. Comput. 33 (2) (2019) 341–345 Apr., doi:10.1007/s10877-018-0151-2.
[10] H.W. Loh, et al., Application of deep learning models for automated identification of Parkinson's disease: a review (2011–2021), Sensors 21 (21) (2021) 7034 Oct., doi:10.3390/s21217034.
[11] B. Mirza, W. Wang, J. Wang, H. Choi, N.C. Chung, P. Ping, Machine learning and integrative analysis of biomedical big data, Genes 10 (2) (2019) 87 (Basel)Jan., doi:10.3390/genes10020087.
[12] H.W. Loh, et al., Automated detection of sleep stages using deep learning techniques: a systematic review of the last decade (2010–2020), Appl. Sci. 10 (24) (2020) 8963 Dec., doi:10.3390/app10248963.
[13] P.Y. Chiang, et al., Machine learning classification for assessing the degree of stenosis and blood flow volume at arteriovenous fistulas of hemodialysis patients using a new photoplethysmography sensor device, Sensors 19 (15) (2019) 3422 Aug., doi:10.3390/s19153422.
[14] Z. Chen, et al., The feasibility of predicting impending malignant ventricular arrhythmias by using nonlinear features of short heartbeat intervals, Comput. Methods Prog. Biomed. 205 (2021) 106102 Jun., doi:10.1016/j.cmpb.2021.106102.
[15] T.Y. Euliano, et al., Photoplethysmography and heart rate variability for the diagnosis of preeclampsia, Anesth. Analg. 126 (3) (2018) 913–919 Mar., doi:10.1213/ANE.0000000000002532.
[16] M.K. Uçar, M.R. Bozkurt, C. Bilgin, K. Polat, Automatic sleep staging in obstructive sleep apnea patients using photoplethysmography, heart rate variability signal and machine learning techniques, Neural Comput. Appl. 29 (8) (2018) 1–16 Apr., doi:10.1007/s00521-016-2365-x.
[17] A. Solosenko, A. Petrenas, V. Marozas, Photoplethysmography-based method for automatic detection of premature ventricular contractions, IEEE Trans. Biomed. Circuits Syst. 9 (5) (2015) 662–669 Oct., doi:10.1109/TBCAS.2015.2477437.
[18] J.G. Lee, et al., Deep learning in medical imaging: general overview, Korean J. Radiol. 18 (4) (2017) 570, doi:10.3348/kjr.2017.18.4.570.
[19] O. Walch, Y. Huang, D. Forger, C. Goldstein, Sleep stage prediction with raw acceleration and photoplethysmography heart rate data derived from a consumer wearable device, Sleep 42 (12) (2019) Dec., doi:10.1093/sleep/zsz180.
[20] Y. Liang, Z. Chen, R. Ward, M. Elgendi, Photoplethysmography and deep learning: enhancing hypertension risk stratification, Biosensors 8 (4) (2018) 101 Oct., doi:10.3390/bios8040101.
[21] R. Huttunen, et al., Assessment of obstructive sleep apnea-related sleep fragmentation utilizing deep learning-based sleep staging from photoplethysmography, Sleep 44 (10) (2021) Oct., doi:10.1093/sleep/zsab142.

[22] M. Radha, et al., A deep transfer learning approach for wearable sleep stage classification with photoplethysmography, NPJ Digit. Med. 4 (1) (2021) 135 Dec., doi:10.1038/s41746-021-00510-8.

[23] D. Moher, A. Liberati, J. Tetzlaff, D.G. Altman, Preferred reporting items for systematic reviews and meta-analyses: the PRISMA statement, PLoS Med. 6 (7) (2009) e1000097 Jul., doi:10.1371/journal.pmed.1000097.

[24] E.S. Väliaho, et al., Wrist band photoplethysmography in detection of individual pulses in atrial fibrillation and algorithm-based detection of atrial fibrillation, EP Eur. 21 (7) (2019) 1031–1038 Jul., doi:10.1093/europace/euz060.

[25] E.S. Väliaho, et al., Wrist band photoplethysmography autocorrelation analysis enables detection of atrial fibrillation without pulse detection, Front. Physiol. 12 (2021) May, doi:10.3389/fphys.2021.654555.

[26] K. Aschbacher, et al., Atrial fibrillation detection from raw photoplethysmography waveforms: a deep learning application, Heart Rhythm O2 1 (1) (2020) 3–9 Apr., doi:10.1016/j.hroo.2020.02.002.

[27] Y.Y. Fan, et al., Diagnostic performance of a smart device with photoplethysmography technology for atrial fibrillation detection: pilot study (Pre-mAFA II registry, JMIR mHealth uHealth 7 (3) (2019) e11437 Mar., doi:10.2196/11437.

[28] S. Kwon, et al., Detection of atrial fibrillation using a ring-type wearable device (CardioTracker) and deep learning analysis of photoplethysmography signals: prospective Observational proof-of-concept study, J. Med. Internet Res. 22 (5) (2020) e16443 May, doi:10.2196/16443.

[29] S.K. Bashar, et al., Atrial fibrillation detection from wrist photoplethysmography signals using smartwatches, Sci. Rep. 9 (1) (2019) 15054 Dec., doi:10.1038/s41598-019-49092-2.

[30] J. Selder, et al., Assessment of a standalone photoplethysmography (PPG) algorithm for detection of atrial fibrillation on wristband-derived data, Comput. Methods Prog. Biomed. 197 (2020) 105753 Dec., doi:10.1016/j.cmpb.2020.105753.

[31] J. Allen, H. Liu, S. Iqbal, D. Zheng, G. Stansby, Deep learning-based photoplethysmography classification for peripheral arterial disease detection: a proof-of-concept study, Physiol. Meas. 42 (5) (2021) 054002 May, doi:10.1088/1361-6579/abf9f3.

[32] F. Fathieh, et al., Predicting cardiac disease from interactions of simultaneously-acquired hemodynamic and cardiac signals, Comput. Methods Prog. Biomed. 202 (2021) 105970 Apr., doi:10.1016/j.cmpb.2021.105970.

[33] U. Hackstein, et al., Early diagnosis of aortic aneurysms based on the classification of transfer function parameters estimated from two photoplethysmographic signals, Inform. Med. Unlocked 25 (2021) 100652, doi:10.1016/j.imu.2021.100652.

[34] D. Ramachandran, V. Ponnusamy Thangapandian, H. Rajaguru, Computerized approach for cardiovascular risk level detection using photoplethysmography signals, Measurement 150 (2020) 107048 Jan., doi:10.1016/j.measurement.2019.107048.

[35] J.L. de Moraes, T.L. de Oliveira, M.X. Rocha, G.G. Vasconcelos, A.R. de Alexandria, Stratification of cardiopathies using photoplethysmographic signals, Inform. Med. Unlocked 20 (2020) 100417, doi:10.1016/j.imu.2020.100417.

[36] J. Wu, H. Liang, C. Ding, X. Huang, J. Huang, Q. Peng, Improving the accuracy in classification of blood pressure from photoplethysmography using continuous wavelet transform and deep learning, Int. J. Hypertens. 2021 (2021) 1–9 Aug., doi:10.1155/2021/9938584.

[37] C.T. Yen, S.N. Chang, C.H. Liao, Deep learning algorithm evaluation of hypertension classification in less photoplethysmography signals conditions, Meas. Control 54 (3–4) (2021) 439–445 Mar., doi:10.1177/00202940211001904.

[38] V.R. Nafisi, M. Shahabi, Intradialytic hypotension related episodes identification based on the most effective features of photoplethysmography signal, Comput. Methods Prog. Biomed. 157 (2018) 1–9 Apr., doi:10.1016/j.cmpb.2018.01.012.

[39] S. Lee, et al., Deep learning models for the prediction of intraoperative hypotension, Br. J. Anaesth. 126 (4) (2021) 808–817 Apr., doi:10.1016/j.bja.2020.12.035.

[40] E. Mejía-Mejía, J.M. May, M. Elgendi, P.A. Kyriacou, Classification of blood pressure in critically ill patients using photoplethysmography and machine learning, Comput. Methods Prog. Biomed. 208 (2021) 106222 Sep., doi:10.1016/j.cmpb.2021.106222.

[41] T. Besleaga, et al., Non-invasive detection of mechanical alternans utilizing photoplethysmography, IEEE J. Biomed. Health Inform. 23 (6) (2019) 2409–2416 Nov., doi:10.1109/JBHI.2018.2882550.

[42] S. Rana, E. Lemoine, J.P. Granger, S.A. Karumanchi, Preeclampsia, Circ. Res. 124 (7) (2019) 1094–1112 Mar., doi:10.1161/CIRCRESAHA.118.313276.

[43] X. Chen, J. Huang, F. Luo, S. Gao, M. Xi, J. Li, Single channel photoplethysmography-based obstructive sleep apnea detection and arrhythmia classification, Technol. Health Care (2021) 1–13 Aug., doi:10.3233/THC-213138.

[44] M.R. Bozkurt, M.K. Uçar, F. Bozkurt, C. Bilgin, In obstructive sleep apnea patients, automatic determination of respiratory arrests by photoplethysmography signal and heart rate variability, Australas. Phys. Eng. Sci. Med. 42 (4) (2019) 959–979 Dec., doi:10.1007/s13246-019-00796-9.

[45] F. Li, et al., Photoplethysmography based psychological stress detection with pulse rate variability feature differences and elastic net, Int. J. Distrib. Sens. Netw. 14 (9) (2018) 155014771880329 Sep., doi:10.1177/1550147718803298.

[46] S. Elzeiny, M. Qaraqe, Automatic and intelligent stressor identification based on photoplethysmography analysis, IEEE Access 9 (2021) 68498–68510, doi:10.1109/ACCESS.2021.3077358.

[47] N.Z. Gurel, H. Jung, S. Hersek, O.T. Inan, Fusing near-infrared spectroscopy with wearable hemodynamic measurements improves classification of mental stress, IEEE Sens. J. 19 (19) (2019) 8522–8531 Oct., doi:10.1109/JSEN.2018.2872651.

[48] A. Kumar, K. Sharma, A. Sharma, Hierarchical deep neural network for mental stress state detection using IoT based biomarkers, Pattern Recognit. Lett. 145 (2021) 81–87 May, doi:10.1016/j.patrec.2021.01.030.

[49] K.S. Na, S.E. Cho, S.J. Cho, Machine learning-based discrimination of panic disorder from other anxiety disorders, J. Affect. Disord. 278 (2021) 1–4 Jan., doi:10.1016/j.jad.2020.09.027.

[50] A.S. Juarascio, R.J. Crochiere, T.M. Tapera, M. Palermo, F. Zhang, Momentary changes in heart rate variability can detect risk for emotional eating episodes, Appetite 152 (2020) 104698 Sep., doi:10.1016/j.appet.2020.104698.

[51] M.H. Hall, R.C. Brindle, D.J. Buysse, Sleep and cardiovascular disease: emerging opportunities for psychology, Am. Psychol. 73 (8) (2018) 994–1006 Nov., doi:10.1037/amp0000362.

[52] A. Zeeck, N. Stelzer, H.W. Linster, A. Joos, A. Hartmann, Emotion and eating in binge eating disorder and obesity, Eur. Eat. Disord. Rev. (2010) p. n/a-n/a, doi:10.1002/erv.1066.

[53] A. Prabha, J. Yadav, A. Rani, V. Singh, Design of intelligent diabetes mellitus detection system using hybrid feature selection based XGBoost classifier, Comput. Biol. Med. 136 (2021) 104664 Sep., doi:10.1016/j.compbiomed.2021.104664.

[54] M.X. Xiao, C.H. Lu, N. Ta, H.C. Wei, B. Haryadi, H.T. Wu, Machine learning prediction of future peripheral neuropathy in type 2 diabetics with percussion entropy and body mass indices, Biocybern. Biomed. Eng. 41 (3) (2021) 1140–1149 Jul., doi:10.1016/j.bbe.2021.08.001.

[55] D.P. Schuster, V. Duvuuri, Diabetes mellitus, Clin. Podiatr. Med. Surg. 19 (1) (2002) 79–107 Jan., doi:10.1016/S0891-8422(03)00082-X.

[56] S. Yagihashi, H. Mizukami, K. Sugimoto, Mechanism of diabetic neuropathy: where are we now and where to go? J. Diabetes Investig. 2 (1) (2011) 18–32 Feb., doi:10.1111/j.2040-1124.2010.00070.x.

[57] H.G. Kang, S. Lee, H.U. Ryu, Y. Shin, Identification of cerebral artery stenosis using bilateral photoplethysmography, J. Healthc. Eng. 2018 (2018) 1–9, doi:10.1155/2018/3253519.

[58] M. Roy Chowdhury, R. Madanu, M.F. Abbod, S.Z. Fan, J.S. Shieh, Deep learning via ECG and PPG signals for prediction of depth of anesthesia, Biomed. Signal Process. Control 68 (2021) 102663 Jul., doi:10.1016/j.bspc.2021.102663.

[59] H. Lim, B. Kim, G.J. Noh, S. Yoo, A deep neural network-based pain classifier using a photoplethysmography signal, Sensors 19 (2) (2019) 384 Jan., doi:10.3390/s19020384.

[60] N. Bourdillon, M. Nilchian, G.P. Millet, Photoplethysmography detection of overreaching, Med. Sci. Sports Exerc. 51 (4) (2019) 701–707 Apr., doi:10.1249/MSS.0000000000001836.

[61] V. Ouyang, et al., The use of multi-site photoplethysmography (PPG) as a screening tool for coronary arterial disease and atherosclerosis, Physiol. Meas. 42 (6) (2021) 064006 Jun., doi:10.1088/1361-6579/abad48.

[62] S. Béres, L. Hejjel, The minimal sampling frequency of the photoplethysmogram for accurate pulse rate variability parameters in healthy volunteers, Biomed. Signal Process. Control 68 (2021) 102589 Jul., doi:10.1016/j.bspc.2021.102589.

[63] J.C. Denny, F.S. Collins, Precision medicine in 2030—seven ways to transform healthcare, Cell 184 (6) (2021) 1415–1419 Mar., doi:10.1016/j.cell.2021.01.015.

[64] M. Kos, X. Li, I. Khaghani-Far, C.M. Gordon, M. Pavel, H.B. Jimison, Can accelerometry data improve estimates of heart rate variability from wrist pulse PPG sensors? in: Proceedings of the 39th Annual International Conference of the IEEE Engineering in Medicine and Biology Society (EMBC), 2017, pp. 1587–1590, doi:10.1109/EMBC.2017.8037141. Jul..

[65] O.S. Lih, et al., Comprehensive electrocardiographic diagnosis based on deep learning, Artif. Intell. Med. 103 (2020) 101789 Mar., doi:10.1016/j.artmed.2019.101789.

[66] S.L. Oh, et al., Classification of heart sound signals using a novel deep WaveNet model, Comput. Methods Prog. Biomed. 196 (2020) 105604 Nov., doi:10.1016/j.cmpb.2020.105604.

[67] S.L. Oh, J. Vicnesh, E.J. Ciaccio, R. Yuvaraj, U.R. Acharya, Deep convolutional neural network model for automated diagnosis of schizophrenia using EEG signals, Appl. Sci. 9 (14) (2019) 2870 Jul., doi:10.3390/app9142870.